



Short communication

# Synthesis and characterization of scandia ceria stabilized zirconia powders prepared by polymeric precursor method for integration into anode-supported solid oxide fuel cells

Hengyong Tu\*, Xin Liu, Qingchun Yu

Institute of Fuel Cell, School of Mechanical Engineering, Shanghai Jiao Tong University, 800 Dong Chuan Road, Shanghai 200240, PR China

## ARTICLE INFO

## Article history:

Received 18 September 2010

Received in revised form

12 November 2010

Accepted 22 November 2010

Available online 26 November 2010

## Keywords:

Intermediate temperature solid oxide fuel cells

Anode-supported

Electrolyte

Scandia-stabilized zirconia

Polymeric precursor method

## ABSTRACT

Scandia ceria stabilized zirconia (10Sc1CeSZ) powders are synthesized by polymeric precursor method for use as the electrolyte of anode-supported solid oxide fuel cell (SOFC). The synthesized powders are characterized in terms of crystalline structure, particle shape and size distribution by X-ray diffraction (XRD), transmission electron microscopy (TEM) and photon correlation spectroscopy (PCS). 10Sc1CeSZ electrolyte films are deposited on green anode substrate by screen-printing method. Effects of 10Sc1CeSZ powder characteristics on sintered films are investigated regarding the integration process for application as the electrolytes in anode-supported SOFCs. It is found that the 10Sc1CeSZ films made from nano-sized powders with average size of 655 nm are very porous with many open pores. In comparison, the 10Sc1CeSZ films made from micron-sized powders with average size of 2.5  $\mu\text{m}$ , which are obtained by calcination of nano-sized powders at higher temperatures, are much denser with a few closed pinholes. The cell performances are 911  $\text{mW cm}^{-2}$  at the current density of 1.25  $\text{A cm}^{-2}$  and 800 °C by application of  $\text{Ce}_{0.8}\text{Gd}_{0.2}\text{O}_2$  (CGO) barrier layer and  $\text{La}_{0.6}\text{Sr}_{0.4}\text{CoO}_3$  (LSC) cathode.

© 2010 Elsevier B.V. All rights reserved.

## 1. Introduction

Solid oxide fuel cells (SOFCs) promise to provide a highly efficient and environmentally friendly method for power generation. Intermediate temperature SOFCs offer important advantages over high temperature SOFCs mainly giving a wider choice of low-cost and high performance materials with a higher stability which will reduce the degradation, increase freedom for structural design, etc. Ytria-stabilized zirconia (YSZ) is the most widely applied electrolyte material for intermediate temperature SOFCs. However, YSZ shows limitations regarding further reduction in the ohmic resistance of the electrolytes. In recent years, scandia stabilized zirconia (ScSZ) materials have attracted significant research attention for the electrolyte application in the intermediate temperature SOFCs due to its much higher ionic conductivity than that of YSZ, the state-of-the-art electrolyte for SOFCs [1]. Co-doping has been proposed with various additional dopants like  $\text{CeO}_2$ ,  $\text{Sm}_2\text{O}_3$ ,  $\text{Yb}_2\text{O}_3$  and  $\text{Al}_2\text{O}_3$  to reduce or prohibit an undesirable phase transition from a high conductive cubic phase to a lower conductive rhombohedral  $\beta$  or tetragonal phase [2–4]. Especially,  $\text{ZrO}_2$  co-doped with  $\text{Sc}_2\text{O}_3$  and  $\text{CeO}_2$  promotes the retention of the cubic phase [5,6]. 10 mol%

$\text{Sc}_2\text{O}_3$ –1 mol%  $\text{CeO}_2$ –89 mol%  $\text{ZrO}_2$  (10Sc1CeSZ) has been adopted as one of the candidate electrolyte materials.

For successful integration of 10Sc1CeSZ electrolyte films into anode-supported SOFCs, a major challenge is fabrication of the dense electrolyte films onto porous anode substrates. Screen-printing is a widely adopted method to fabricate electrolyte films, which is cost effective and suitable for mass production. A dense and almost pore-free YSZ film can be achieved on the Ni/YSZ cermet substrate after sintering [6]. It was reported that the characteristics of YSZ powders has a significant effect on the formation of dense YSZ films on anode substrates for the development of intermediate temperature SOFCs [7,8]. The ScSZ powders were synthesized by several techniques such as solid-state reaction [9], co-precipitation [10], sol-gel [11] and glycine nitrate process [12]. Further synthesis technique deserves exploration for production of large quantities of high purity 10Sc1CeSZ powders suitable for fabrication of the electrolyte films in anode-supported SOFCs. In the present study, 10Sc1CeSZ powders were synthesized by polymeric precursor method (Pechini method) [13]. The polymeric precursor method is known to employ complexing of cations in organic media, making use of low cost precursors resulting in a homogeneous ion distribution at molecular level, which facilitates synthesis of the crystallized powder with ultrafine particle size and high purity at low temperature. 10Sc1CeSZ electrolyte films on green anode substrate were deposited by screen-printing method.

\* Corresponding author. Tel.: +86 21 34206249; fax: +86 21 34206249.

E-mail address: [hytu@sjtu.edu.cn](mailto:hytu@sjtu.edu.cn) (H. Tu).

Effects of 10Sc1CeSZ powder characteristics on sintered films were investigated regarding the integration process for application as the electrolytes in anode-supported SOFCs.

## 2. Experimental

### 2.1. Synthesis

The starting materials used in the synthesis of 10Sc1CeSZ powders were  $\text{Sc}(\text{NO}_3)_3$  (99.99%),  $\text{Ce}(\text{NO}_3)_3 \cdot 6\text{H}_2\text{O}$  (AR),  $\text{Zr}(\text{NO}_3)_4 \cdot 5\text{H}_2\text{O}$  (AR), citric acid (AR) and ethylene glycol (AR), all from Sinopharm Chemical Reagent Co. Ltd, China. The polymeric precursor solution was prepared by adding citric acid and ethylene glycol into the aqueous solution with  $\text{Sc}(\text{NO}_3)_3$ ,  $\text{Ce}(\text{NO}_3)_3 \cdot 6\text{H}_2\text{O}$  and  $\text{Zr}(\text{NO}_3)_4 \cdot 5\text{H}_2\text{O}$  at room temperature. The molar ratio metal/citric acid/ethylene glycol was chosen as 1/4/16. With continued heating, the solution became more viscous and a gel was formed. The gel was dried at 200 °C in air during a night and solidified into dark-brown glassy resin. Charring the resin at 400 °C for 2 h resulted in a dark-brown solid mass. The powder obtained at this stage is referred to as “precursor powder”. The powders were heat-treated at 700 °C for 6 h in air. Some of the nano-sized 10Sc1CeSZ powders were calcined at 1000–1400 °C in order to obtain micro-sized powders. The calcined 10Sc1CeSZ powders were subject to ball milling in ethanol for 24 h using zirconia balls. Similarly,  $\text{Ce}_{0.8}\text{Gd}_{0.2}\text{O}_2$  (CGO) powders were synthesized from polymeric precursor solution using  $\text{Ce}(\text{NO}_3)_3 \cdot 6\text{H}_2\text{O}$  (AR),  $\text{Gd}(\text{NO}_3)_3 \cdot 6\text{H}_2\text{O}$  (AR), citric acid (AR) and ethylene glycol (AR) as the starting materials, all from Sinopharm Chemical Reagent Co. Ltd, China. The powders were heat-treated at 700 °C for 6 h in air.  $\text{La}_{0.6}\text{Sr}_{0.4}\text{Co}_{0.2}\text{Fe}_{0.8}\text{O}_3$  (LSCF) and  $\text{La}_{0.6}\text{Sr}_{0.4}\text{CoO}_3$  (LSC) were prepared by a glycine nitrate process (GNP) process [14].

### 2.2. Characterization

Thermogravimetric analysis (TGA) was done in a TA Instruments at a heating rate of 10 °C min<sup>-1</sup> in air flow. The resultant phases were analyzed by X-ray powder diffraction (XRD) using Cu K $\alpha$  radiation and a graphite monochromator (40 kV, 40 mA) (Model MXP, MAC, Japan). The mean crystallite size was calculated with the Scherrer equation. The morphology of powders was evaluated using transmission electron microscopy (TEM, JEM-2010). Particle size distributions were measured using photon correlation spectroscopy (PCS, Zetasizer Nano S). The microstructure was observed using field emission scanning electron microscopy (FE-SEM, Hitachi 6300).

### 2.3. Fabrication

The anode-supported cells adopt the standard NiO/YSZ as anode substrate, NiO/10Sc1CeSZ as anode function layer, 10Sc1CeSZ as electrolyte, CGO as barrier layer and LSCF/CGO or LSC as cathode. Planar NiO/YSZ anode supports were fabricated by tape casting. The starting materials of the anode supports were composed of NiO (Nickelous Oxide Green, Sinopharm Chemical Reagent Co. Ltd, China), YSZ (TZ-8YS, Tosoh Co., Japan) with a weight ratio of 60/40. 20 wt% of cornstarch powders were added as pore former. The NiO, YSZ and cornstarch powders were mixed with the solvents (ethanol and butanone), dispersants (triethyl phosphate), binders (polyvinyl butyral) and plasticizers (polyethylene glycol and dibutyl phthalate) by a ball milling process for 24 h. The slurry was cast on a moving PET film using a tape-casting machine after deair. After tape-casting and evaporation of the dispersion aid, the resulting green tape was cut in the appropriate dimension. The NiO/10Sc1CeSZ anode function layer was deposited on the surface of the green anode support by screen printing. Subsequently, the 10Sc1CeSZ electrolyte films from nano-sized or micron-sized

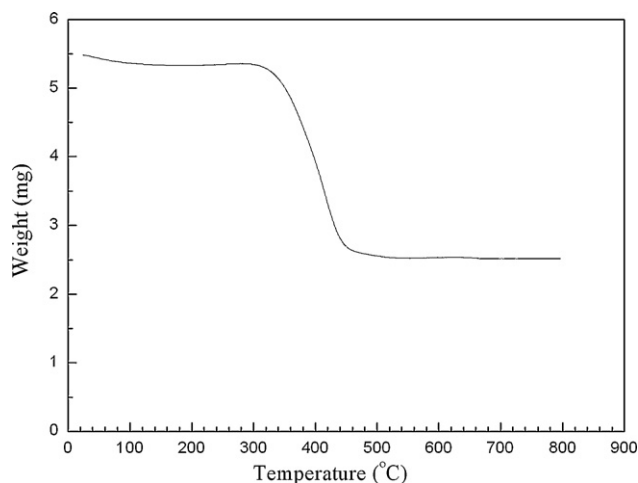


Fig. 1. TG curve for the 10Sc1CeSZ precursor powders.

powders were applied by screen printing. Half cells were then co-sintered at 1450 °C for 4 h in air. The CGO barrier layers were applied on 10Sc1CeSZ by screen printing. Sintering of the barrier layers was carried out at 1300 °C in air for 1 h. Finally, the cathode films of LSCF/CGO or LSC were applied on the barrier layers by screen printing and sintered at 950–1000 °C in air for 2 h. Cornstarch was used as pore former in the cathode formulation. The single cells have the approximate size of 5 cm × 5 cm. The cathode has the dimension of 3.2 cm × 3.2 cm.

### 2.4. Performance testing

The cell performances were evaluated with a fuel cell test station (SF10, Lixin, Wuhan, China). Nickel (Ni) and platinum (Pt) meshes were used for current collection on anode and cathode sides, respectively. The single cells were sealed with a silver paste. A weight of 7 kg was placed on top of the cell housing for a better contact between the current collectors and the electrodes. The gas flows to the anode and the cathode were controlled by digital mass flow controllers. The anode side was flushed with humidified (3% H<sub>2</sub>O) hydrogen with a flow rate of 1000 ml min<sup>-1</sup>. On the cathode side, air was supplied as oxidant with a flow rate of 2000 ml min<sup>-1</sup>. The current density and voltage values were recorded as a function of operating temperatures in the range 600–800 °C. Before testing, the cell was operated at the voltage of 0.75 V for 3 h.

## 3. Results and discussion

The thermogravimetric analysis from room temperature to 900 °C was performed in order to determine the appropriate heat treatment condition of the 10Sc1CeSZ precursor powders. As shown in Fig. 1, there are two main weight loss phases in the whole temperature range. The first weight loss related to water appears at 100 °C. The pyrolysis of organic materials occurs at temperatures between 300 and 520 °C. After that, no weight loss can be detected because the decomposition of organic material has finished. Taking into account these results and complete formation of pure phase cubic fluorite structure, the 10Sc1CeSZ precursor powders were calcined at 700 °C.

As shown in Fig. 2, XRD analysis of the calcined 10Sc1CeSZ powders revealed the peaks expected from the cubic phase without any other phases, which indicated that 10Sc1CeSZ powders could be successfully synthesized by the polymeric precursor method. Fig. 2 shows XRD patterns of 10Sc1CeSZ powders after calcination of the as-synthesized powders at different temperatures. The high

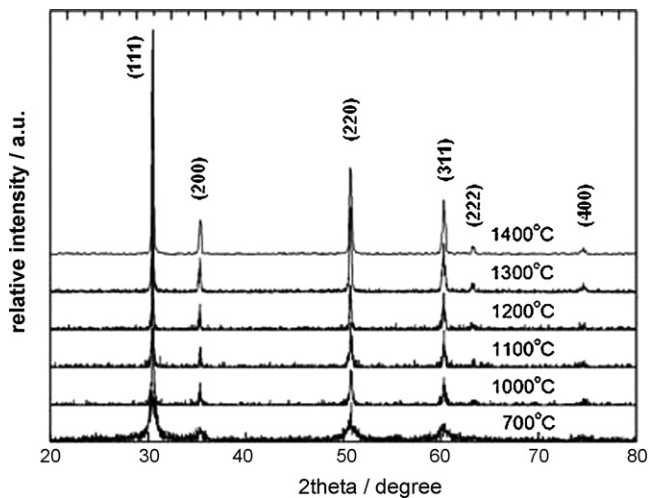


Fig. 2. XRD patterns of the 10Sc1CeSZ powders calcined at different temperatures.

temperature cubic phase of 10Sc1CeSZ could be stabilized to that of room temperature, and no trace of rhombohedral-ZrO<sub>2</sub> phase could be detected. Therefore, inhibition of cubic–rhombohedral phase transformation assures integration process of 10Sc1CeSZ electrolytes into anode-supported SOFCs. The line broadening in the X-ray diffraction peaks of the as-synthesized 10Sc1CeSZ powders clearly indicates the formation of nano-crystallites. Based on the Scherrer equation, the mean crystallite size was calculated to be about 18.6 nm using the (1 1 1) reflection. In addition, the narrowing of the diffraction peak width with increasing calcination temperature shows that the crystallite size of the nanocrystals increases prominently with the temperature. The peaks gradually sharpen with increasing calcination temperature, which indicates an increase of crystallinity.

TEM analyses of as-synthesized powders were performed. As an example, Fig. 3 shows the TEM micrograph of 10Sc1CeSZ powders calcined at 700 °C. It was observed that the nanoparticles are tightly agglomerated and size of the nanoparticles is around 20 nm, which corroborates well with the X-ray line broadening studies. TEM analyses indicate that a particle is an agglomerate of primary particles that are single crystallites. In an agglomerate, the primary particles

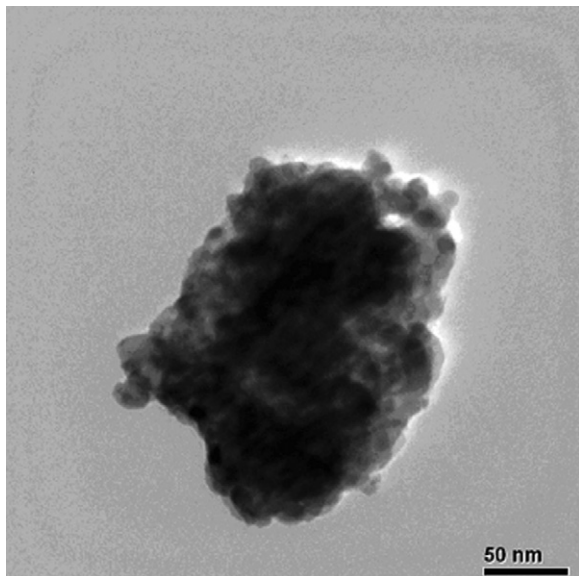


Fig. 3. Transmission electron microscopic micrograph of the 10Sc1CeSZ powders calcined at 700 °C.

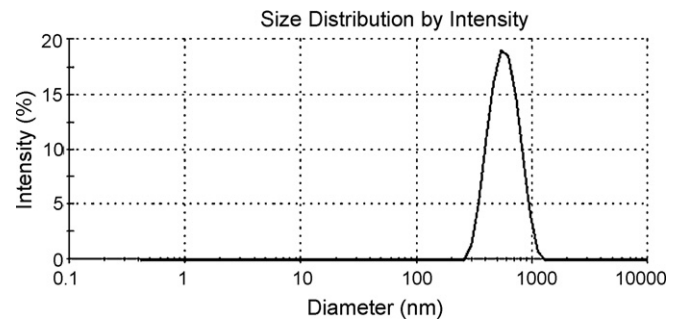
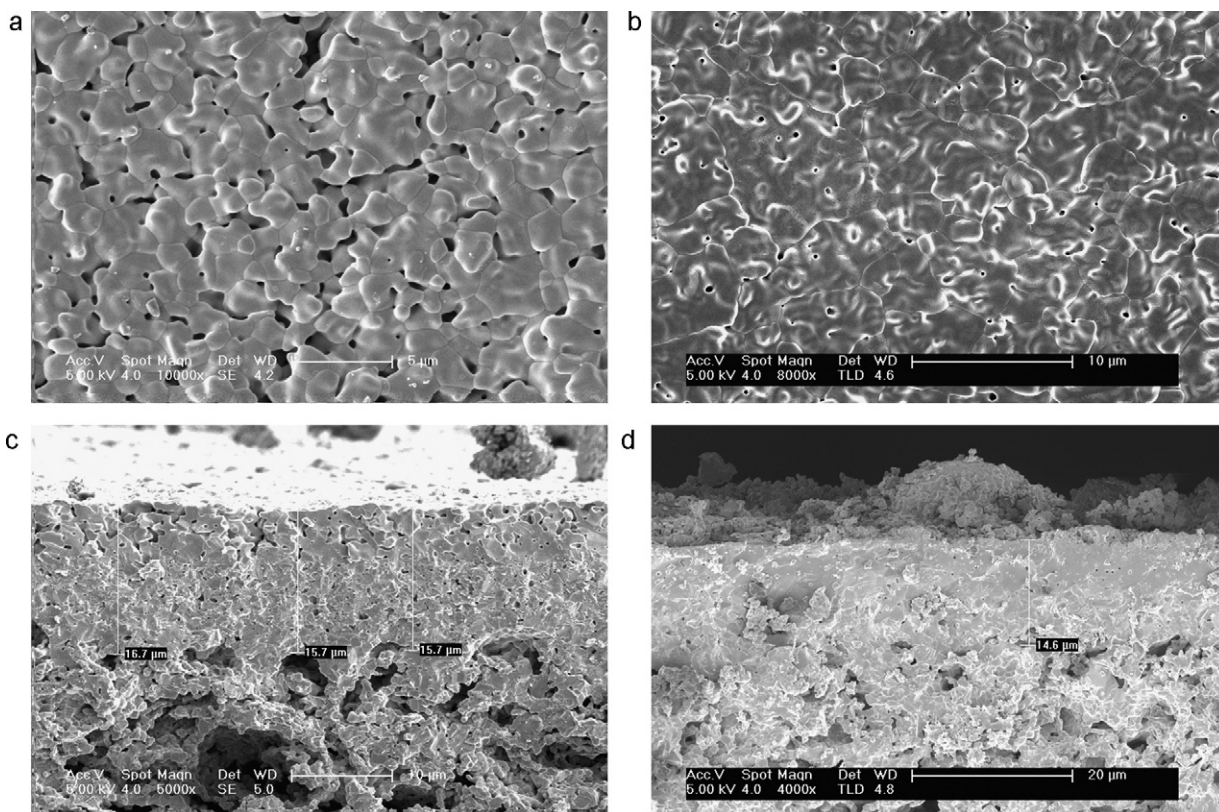


Fig. 4. Size distribution of the 10Sc1CeSZ agglomerated particles measured by photon correlation spectroscopy (PCS).

are bonded together by forming necks at the active contact points [15]. Measurements by photon correlation spectroscopy (PCS) indicated a narrow size distribution of the agglomerated particles, as shown in Fig. 4. The average particle size is about 650 nm.

Gas-tight electrolyte films to separate air and fuel gas are expected for successful integration of 10Sc1CeSZ powders prepared by polymeric precursor method into anode-supported SOFCs. Preparation of dense electrolyte films on porous electrodes is an important step in the fabrication of high-performance SOFCs. For the investigation of the co-sintering behaviors of the 10Sc1CeSZ electrolyte film, NiO/10Sc1CeSZ film and 10Sc1CeSZ film were screen-printed on the surface of green NiO/YSZ support in succession. After printing, the three green layers were dried and co-sintered at 1450 °C for 4 h. The sintered half cells exhibited good flatness, and the films attached well to the substrate. It was found that the nano-sized powders calcined at 700 °C only allowed a lower solid loading for a printable paste, which resulted in the low green density of the deposited 10Sc1CeSZ film. According to Shi [16], if the green density of ceramics is lower than a critical value, namely, ~33%, it is difficult to reach full densification under pressureless solid-state sintering conditions due to the existence of thermodynamically stable large pores. On co-sintering of the 10Sc1CeSZ electrolyte film made of nano-sized powders, NiO/10Sc1CeSZ film and the anode support, the low green density of the 10Sc1CeSZ film would make the densification of the electrolyte film difficult despite the high sintering temperature of 1450 °C. Micrographs of the surface and cross-section of the 10Sc1CeSZ electrolyte films made of nano-sized powders are shown in Fig. 5a and c. The 10Sc1CeSZ film prepared from nano-sized powders is very porous with many open pores in the surface and in the cross-section of films. Thus higher green density of the 10Sc1CeSZ film was expected using micro-sized 10Sc1CeSZ powders for screen printing process. As shown in Fig. 2, the crystallite sizes apparently increase after calcination in the temperature range of 1000–1400 °C. Micro-sized 10Sc1CeSZ powders with average particle size of 2.5 μm from PCS measurement were obtained just through calcination of nano-sized powders at 1000 °C for 4 h. In comparison, the micro-sized powders allowed a higher solid loading than the nano-sized powders while still obtaining a printable paste. Easier densification of the 10Sc1CeSZ film made of micro-sized powders would be expected during the same co-sintering process. Micrographs of the surface and cross-sections of the 10Sc1CeSZ electrolyte films made of micron-sized powders are shown in Fig. 5b and d. The thickness of both the electrolyte films is ca. 15 μm (Fig. 5c and d). In comparison, the 10Sc1CeSZ film made from micron-sized powders is much denser with a few closed pinholes. Furthermore, the 10Sc1CeSZ film from micro-sized powders presents no apparent crack formation after co-sintering with anode substrate and function layer. This result revealed that the characteristics of the starting powders had crucial effect on the densification of the screen-printed 10Sc1CeSZ films during co-sintering.





**Fig. 5.** Comparison of surface and cross-section microstructures of the 10Sc1CeSZ films made of nano-sized powders (a, c) and micron-sized powders (b, d) after sintering at 1450 °C.

Fig. 6 shows comparison of the open-circuit voltages (OCVs) of anode-supported cells with the 10Sc1CeSZ electrolyte films made of nano-sized and micro-sized powders, respectively. Here the cathode LSCF/CGO was not optimized and used only for OCV measurements. Both cells were tested under the same gas conditions. The OCVs of the cell with the 10Sc1CeSZ electrolyte film made of micron-sized powders were significantly higher than that made of nano-sized powders. For example, the OCV of the former at 800 °C was 1.08 V, while this value was only 0.82 V for the latter. There was a gap of more than 0.22 V between the OCVs of the two cells in the temperature range of 600–800 °C. The lower OCVs of the cell with the 10Sc1CeSZ electrolyte film made of nano-sized powders indicated some cross-over of fuels, which clearly confirmed that the pores in the electrolyte film made of nano-sized powders were penetrated. In comparison, the cells with the 10Sc1CeSZ electrolyte film made of micro-sized powders achieved high OCVs,

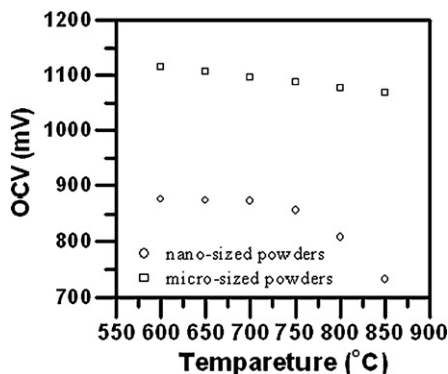


**Fig. 6.** Comparison of OCV of anode-supported cells with the 10Sc1CeSZ electrolyte films made of nano-sized and micron-sized 10Sc1CeSZ powders.

which confirmed that these 10Sc1CeSZ electrolyte films were sufficiently dense.

The performance of the single cell was shown in Fig. 7. The cell was operated with 97% H<sub>2</sub> + 3% H<sub>2</sub>O gas as a fuel and air as an oxidant gas. It exhibited the OCVs of 1.098 V, 1.115 V and 1.133 V at 800 °C, 700 °C and 600 °C, respectively. Clearly the OCV values revealed that the 10Sc1CeSZ electrolyte films were dense enough to avoid the gas leakage. Nano-sized LSC powders synthesized by GNP were applied as cathode of the single cell. The powders exhibited the BET-specific area of 10.4 m<sup>2</sup> g<sup>-1</sup> [14]. CGO films were applied as barrier layers between 10Sc1CeSZ and LSC films in order to prevent formation of an insulating SrZrO<sub>3</sub>. The CGO film was porous after sintering at 1300 °C due to the low sintering activity of CGO, as shown in Fig. 8. Testing results showed that relatively good performances were obtained. At the current density of 1.25 A cm<sup>-2</sup>, the power density of the cell at 800 °C and 700 °C reached 911 mW cm<sup>-2</sup> and 729 mW cm<sup>-2</sup>, respectively. In

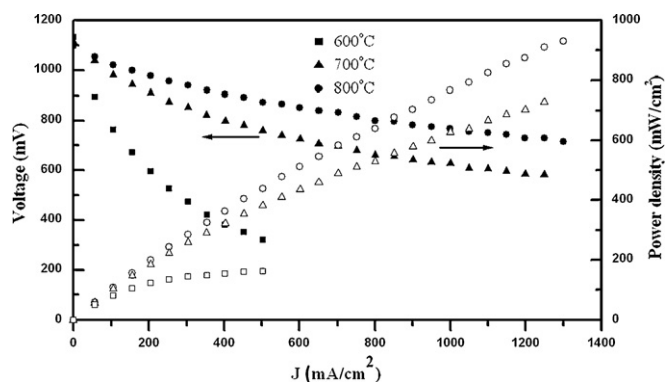


**Fig. 7.** Performance of a single cell with integration of 10Sc1CeSZ electrolyte.

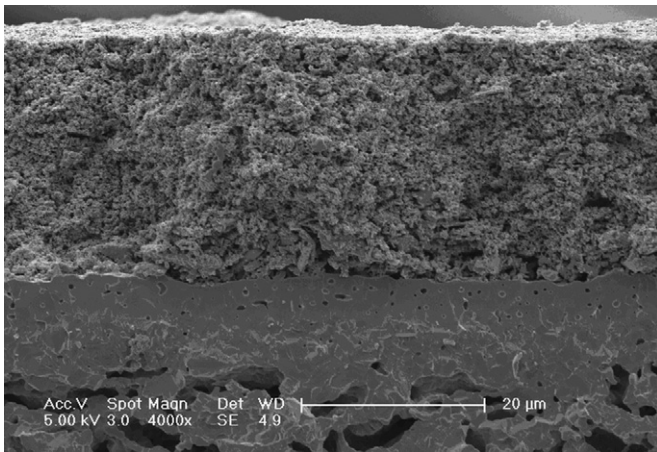


**Fig. 8.** SEM image for the cross-section of a single cell with the LSC cathode sintered at 950 °C.

comparison, the power density at 600 °C reduced significantly and reached only  $161 \text{ mW cm}^{-2}$  at the current density of  $0.5 \text{ A cm}^{-2}$ . These results suggest that low sintering temperature of LSC can prevent  $\text{SrZrO}_3$  formation although GCO barrier layer exhibited porous structure. At the same time, the growth in particles size of LSC powders can be inhibited at low sintering temperature, leading to more triple phase boundary points.

#### 4. Conclusion

Applicability of the polymeric precursor method has been demonstrated for production of nano-sized 10Sc1CeSZ powders. Micro-sized 10Sc1CeSZ powders can be obtained just through calcination of the nano-sized powders at 1000 °C. Dense 10Sc1CeSZ films made of micro-sized powders were successfully obtained by screen-printing process and co-sintering with green anode support and functional layer. In comparison, the 10Sc1CeSZ film prepared

from nano-sized powders exhibited penetrated porous microstructure. The result indicated that the characteristics of the starting powders had crucial effect on the densification of the screen-printed 10Sc1CeSZ films during co-sintering. The power density of  $911 \text{ mW cm}^{-2}$  (at the current density of  $1.25 \text{ A cm}^{-2}$ , at 800 °C) was achieved in combination with CGO barrier film and LSC cathode. Combination of polymeric precursor method with screen printing technology provides a simple and cost-effective way to fabricate dense 10Sc1CeSZ electrolyte films on porous anode supports.

#### Acknowledgement

This work was financially supported by the European Commission under contract no. SES6-CT-2006-020089 as part of the Integrated Project “SOFC600”.

#### References

- [1] O. Yamamoto, Y. Arati, Y. Takeda, N. Imanishi, Y. Mizutani, M. Kawai, Y. Nakamura, *Solid State Ionics* 79 (1995) 137.
- [2] Y. Arachi, T. Asai, O. Yamamoto, Y. Takeda, N. Imanishi, K. Kawate, C. Takakoshi, *J. Electrochem. Soc.* 148 (2001) A520.
- [3] T. Ishii, *Solid State Ionics* 78 (1995) 333.
- [4] K. Ukai, Y. Mizutani, Y. Kume, in: H. Yokogawa, S.C. Singhal (Eds.), *Proc. of the 7th Int. Symposium on Solid Oxide Fuel Cells*, The Electrochem. Soc. Inc., NJ (2001) 375.
- [5] Z. Wang, M. Cheng, Z. Bia, Y. Dong, H. Zhang, J. Zhang, Z. Feng, C. Li, *Mater. Lett.* 59 (2005) 2579.
- [6] M.A. Laguna-Bercero, S.J. Skinner, J.A. Kilner, *J. Power Sources* 192 (2009) 126.
- [7] Y. Zhang, X. Huang, Z. Lü, X. Ge, J. Xu, X. Xin, X. Sha, W. Su, *Solid State Ionics* 177 (2006) 281.
- [8] Y. Jun Leng, S. Hwa Chan, K. Aik Khor, S. Ping Jiang, P. Cheang, *J. Power Sources* 117 (2003) 26.
- [9] R. Ruh, H.J. Garrett, R.F. Domagala, V.A. Patel, *J. Am. Ceram. Soc.* 60 (1977) 399.
- [10] S.P.S. Badwal, J. Drennan, *Solid State Ionics* 53–56 (1992) 769.
- [11] Y. Mizutani, M. Tamura, M. Kawai, O. Yamamoto, *Solid State Ionics* 72 (1994) 271.
- [12] D. Lee, I. Lee, Y. Jeon, R. Song, *Solid State Ionics* 176 (2005) 1021.
- [13] M.P. Pechini, U.S. Patent 3,330,697 (1967).
- [14] H.-x. Wang, H.-y. Tu, *J. Funct. Mater.* 41 (3) (2010) 397.
- [15] R.K. Lenka, T. Mahata, P.K. Sinha, B.P. Sharma, *J. Am. Ceram. Soc.* 89 (2006) 3871.
- [16] J.L. Shi, *J. Mater. Res.* 14 (1999) 1398.